A&A manuscript no.
(will be inserted by hand later)

Your thesaurus codes are:
04 (04.01.1; 04.03.1; 13.07.1)

ASTRONOMY
AND
ASTROPHYSICS
5.2.2008

arXiv:astro-ph/9708156v1 18 Aug 1997

GRANAT/WATCH catalogue of cosmic gamma-ray bursts: December 1989 to September 1994*

S.Y. Sazonov[1,2], R.A. Sunyaev[1,2], O.V. Terekhov[1], N. Lund[3], S. Brandt[4] and A.J. Castro-Tirado[5]

[1] Space Research Institute, Russian Academy of Sciences, Profsoyuznaya 84/32, 117810 Moscow, Russia
[2] Max-Planck-Institut für Astrophysik, Karl-Schwarzschildstr 1, 85740 Garching, Germany
[3] Danish Space Research Institute, Juliane Maries Vej 30, DK 2100 Copenhagen Ø. Denmark
[4] Los Alamos National Laboratory, MS D436, Los Alamos, NM 87545, USA
[5] Laboratorio de astrofísica Espacial y Física Fundamental (LAEFF), INTA, P.O. Box 50727, 28080 Madrid, Spain

Received May 1997; accepted August 1997

Abstract. We present the catalogue of gamma-ray bursts (GRB) observed with the WATCH all-sky monitor on board the GRANAT satellite during the period December 1989 to September 1994. The cosmic origin of 95 bursts comprising the catalogue is confirmed either by their localization with WATCH or by their detection with other GRB experiments. For each burst its time history and information on its intensity in the two energy ranges 8–20 keV and 20–60 keV are presented. Most events show hardening of the energy spectrum near the burst peak. In part of the bursts an X-ray precursor or a tail is seen at 8–20 keV. We have determined the celestial positions of the sources of 47 bursts. Their localization regions (at 3σ confidence level) are equivalent in area to circles with radii ranging from 0.2 to 1.6 deg. The burst sources appear isotropically distributed on the sky on large angular scales.

Key words: astronomical data bases: miscellaneous – catalogs – gamma rays: bursts

1. Introduction

From December 1989 to September 1994 the astrophysical observatory GRANAT performed pointed observations of different celestial regions. During that period, the X-ray instrument WATCH, a part of the scientific payload of the observatory, was monitoring the whole of the sky. WATCH is uniquely capable of precisely measuring the celestial positions (the radius of the localization region is generally smaller than 1 deg at the 3σ confidence level) of short-lived hard X-ray sources, which include GRBs. Another feature of the instrument relevant to observations of GRBs is that its detectors are sensitive over an X-ray energy range that reaches down to ~ 8 keV, the domain where the properties of GRBs are known less than at higher energies.

In this paper, we present the catalogue of GRBs detected with WATCH in 1989–1994. For nearly half of the events we have been able to determine the location of the burst source on the celestial sphere. Earlier, a preliminary catalogue covering the WATCH observations carried out before October 1992 was compiled by Castro-Tirado (1994). The new catalogue has been updated mainly in the two aspects: 1) the bursts detected between October 1992 and September 1994 have been added, 2) more accurate positions have been determined for many of the previously catalogued events due to the use of more precise information on the spacecraft attitude and an improved model of the instrument.

2. The WATCH experiment

Four monitors WATCH (Lund 1986), designed at the Danish Space Research Institute, are mounted on board the orbital observatory GRANAT. The field of view of a monitor is a circle 74° radius. The scintillation detector is made of alternating stripes of NaI and CsI. The full geometrical area of the detector is 47 cm^2. The effective area of the detector is dependent on the incident angle of the arriving photons as shown in Fig. 1: at small angles it declines as a cosine, starting at $\sim 52°$ more steeply, and for a source 65° off-axis it is one fourth of that for an on-axis source. The fields of view of the four instruments cover different quarters of the sky and partially overlap. Because at

---

Send offprint requests to: S.Y. Sazonov (sazonov@hea.iki.rssi.ru)

* Figure 2 is only available in the on-line version of the paper; Table 1 is only available in electronic form at the CDS via anonymous ftp to cdsarc.u-strasbg.fr (130.79.128.5) or via http://cdsweb.u-strasbg.fr/Abstract.html

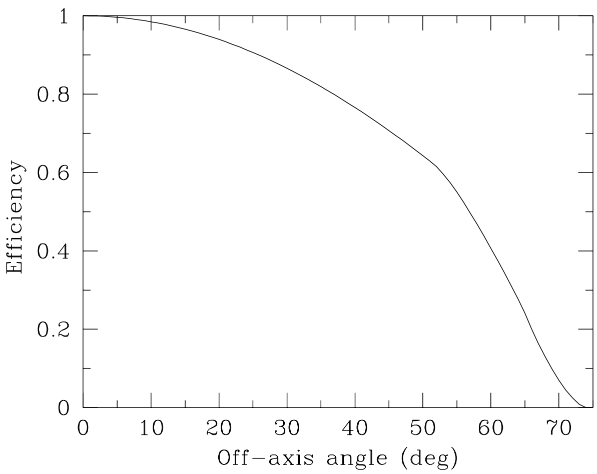

Fig. 1. Detector efficiency as a function of source off-axis angle (same for both WATCH energy bands)

the very beginning of the experiment one of the monitors went out of order, ∼ 80 % of the sky can be simultaneously viewed under most favourable conditions. The performance of the WATCH instrument is based on the rotation modulation collimator principle. A point source, provided it is bright enough for at least one rotation of the modulation collimator (∼ 1 s), can be localized with an accuracy of $\sim 50/n_{10}$ arcmin (at the 3σ confidence level), where n_{10} is the source signal in units of 10 standard deviations (Brandt 1994). The detector count rate is recorded in two energy bands, the boundaries of which were reset several times during the mission and roughly correspond to 8–20 keV and 20–60 keV.

3. Registration of cosmic gamma-ray bursts

WATCH possesses an on-board algorithm of triggering on burst events. A burst is detected if an increase in the count rate of more than 6 standard deviations above the background level has been registered at one of 12 sampling times evenly covering on the logarithmic scale a range from 16 ms to 32 s. If an event is detected on a time scale shorter than 2 s, its time history will be recorded with a resolution of 1 s, whereas for slower bursts the standard integration time of either 7 s or 14 s will be used. The purpose of the ground data analysis is then to separate events of cosmic and different nature. These latter include solar flares which differ from GRBs in their generally softer spectra. It is also usually possible to establish with WATCH that their incident direction is coincident with the direction to the solar disc. In many cases burst events were generated by accelerated charged particles. The time histories of such events are different from those of GRBs. Although most non-cosmic events can be reliably identified by their characteristic features, the origin of a number of bursts remains unsettled. In this catalogue, only those events are presented that either have been localized with WATCH or are designated as cosmic in the catalogues of other GRB experiments. The significance of the detection of ∼ 25 % of the bursts included in the catalogue was not high enough (6σ) to generate a trigger on board. These events, discovered already in the course of the ground analysis as a significant ($> 4\sigma$) increase in the count rate, are coincident in time with GRBs observed by other experiments, mainly by the BATSE instrument on the Compton Gamma-Ray Observatory (Meegan et al. 1996).

4. The catalogue

A total of 95 GRBs have been included in the catalogue. The information on these events is presented in Table 1. In the first column of the table the names of the bursts are given, which were formed using a common terminology: the first letter 'W' indicates the instrument's name, WATCH, then follows the year, month and day of the detection of the event. The burst may have a letter ('b' or 'c') appended to its name, if it is the second or third burst detected in a day. The second column yields the time (UT) of the trigger. In the subsequent columns the basic characteristics of the bursts are given. As a measure of the burst duration we use the quantity T_{90} which is the length of the interval during which 90 % (from 5 % to 95 %) of the total counts from a burst was accumulated. The fluence and the peak energy flux of the bursts were calculated in the two energy bands: 8–20 keV and 20–60 keV (spectral shape similar to that of the Crab Nebula was assumed). When calculating these quantities we made a correction for the aspect of the burst source, which is known for the majority of the presented events from localizations with either WATCH or CGRO/BATSE (Meegan et al. 1996). However, for 18 bursts such information is not available, hence we accepted for them as an estimate of the detector geometrical efficiency (see Fig. 1) its expectation value of 0.7. The quoted errors for the fluxes are purely statistical ones, the uncertainties due to unknown spectral shapes and source aspects have not been considered. The peak flux was calculated using the count rate data with the best time resolution available for a given event. Also, given in the table is the ratio of the fluences in the 20–60 keV and 8–20 keV energy bands, which characterizes the hardness of the burst spectrum. Finally, the last column of the table contains information on detections of the bursts by other experiments that were in orbit during the period examined: KONUS/GRANAT, PHEBUS/GRANAT, SIGMA/GRANAT, GINGA, BATSE/CGRO, COMPTEL/CGRO, OSSE/CGRO, DMS, Mars Observer, PVO, ULYSSES, WATCH/EURECA and YOHKOH (Golenetskii et al. 1991; Terekhov et al. 1994; Terekhov et al. 1995; Sunyaev et al. 1993; Ogasaka et al. 1991; Meegan et al. 1996;

Hanlon et al. 1994; Hurley et al. 1994; Brandt et al. 1994).

4.1. Burst time histories

In Fig. 2 the time histories of the detector count rate during the bursts in the two WATCH energy bands are shown. For the longer bursts, the best time resolution available is either 7 s or 14 s. For the shorter events, time histories of 1 s resolution are presented. Finally, for the two shortest events W900404 and W930106, which lasted less than 1 s, light curves obtained by integrating the count rate over 20 ms intervals are presented. We note that these two time histories are necessarily distorted to some degree by the modulation effect caused by the rotation of the collimator. The background was in most cases estimated by averaging the count rate over time intervals immediately before and after the burst. When the background was strongly variable during the burst, we used approximation of the count rate by polynomials of first or higher orders.

4.2. Burst durations

Figure 3 shows the duration (T_{90}) distribution for the bursts detected. It was obtained using those 89 out of 95 events whose durations could be determined reliably. At least 5 of the 6 events excluded from the analysis are apparently short (shorter than a few seconds), but they were too weak to force the on-board burst logic to trigger. Hence no count rate data with a good time resolution needed for determining their durations is available. The mean burst duration is 66 s, and the maximum of the distribution lies in the interval 10 to 100 s. Our sample contains 2 events shorter than 2 s and 7 events longer than 200 s. In other experiments, two classes of bursts were identified: of duration shorter and longer than $\sim$ 2 s (Kouveliotou et al. 1993). It was noticed that the energy spectra of the shorter bursts of type 1 were generally harder than those of the longer bursts of type 2 (Kouveliotou et al. 1993; Lestrade et al. 1993). The negligibly small number of type 1 events in our catalogue compared to the previous results (Meegan et al. 1996; Terekhov et al. 1995) can be accounted for by at least two selectional effects: 1) all bursts with detection significance less than 6σ included in our duration sample are longer than 7 s, because this value is the time resolution of the data, 2) WATCH is sensitive to X-ray photons with energies significantly below the effective energy of the photons emitted in type 1 bursts.

4.3. Burst spectral hardness and evolution

The spectral information on the emission produced during GRBs provided by WATCH is limited to the count rates in the two energy ranges 8–20 keV and 20–60 keV. Hence to describe the spectra of the observed bursts we calculated the ratios of the burst energy fluxes in the higher and lower bands. As follows from the cross-correlation diagram presented in Fig. 4, there is no clear dependence of burst overall hardness ratio (the 20–60 keV fluence divided by the 8-20 keV fluence) on burst duration. This graph gives further support to the above statement that most of the bursts in the WATCH catalogue are of the same type.

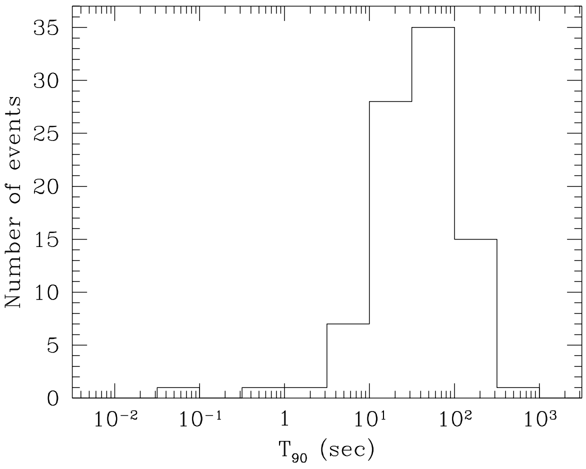

Fig. 3. Histogram of durations (T_{90}) for the WATCH bursts

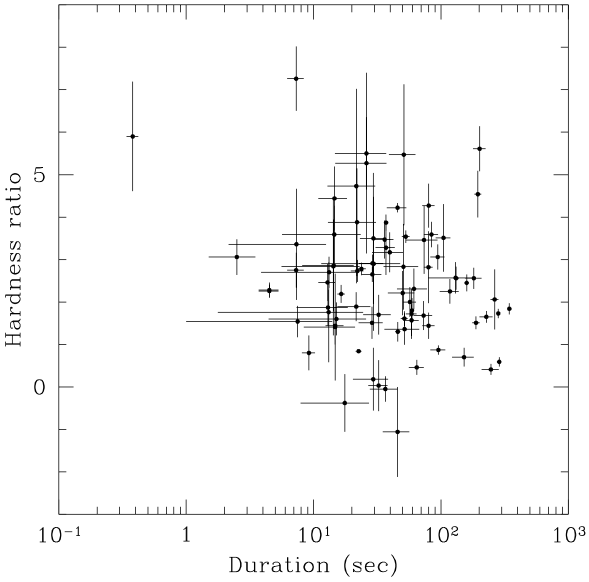

Fig. 4. Burst hardness ratios (fluence over the 20–60 keV band divided by that over the 8–20 keV band) vs. burst durations

The WATCH observations illustrate that the energy spectra are usually not constant but evolve throughout bursts, the typical situation being that the spectra during the burst rise and decay phases are softer than that at the peak of the event. This is demonstrated by Fig. 5, where burst peak hardness ratio, i.e. the ratio of the peak energy fluxes in 20–60 keV and 8–20 keV (in some bursts the two flux maxima are not coincident in time), is shown as a function of burst overall hardness ratio. It can be seen that the former is larger than the latter for the majority of events, reflecting the fact that bursts generally have "sharper" profiles in the harder energy band. In 13 bursts (Table 2) this spectral evolution reveals itself especially distinctly as a significant activity observed only at 8–20 keV either preceding or following the hard X-ray event (see the corresponding time histories in Fig. 2, for discussion on part of these events with occurences before October 1992 see also Castro-Tirado (1994) and Castro-Tirado et al. (1994)). Similar X-ray precursor and tail activities have been observed before in a number of bursts by a few space-flown GRB instruments sensitive to medium or soft X rays (Murakami et al. 1991). In the observations carried out with the GRB detector on board the GINGA satellite, which had a low-energy cut-off at as low as 1.5 keV, such X-ray-active events accounted to about one third of the total bursts detected (Murakami et al. 1992). The photon spectra measured with GINGA at 1 to 10 keV during both the burst X-ray precursor and tail could be approximated by a black-body model with temperatures between 1 and 2 keV, indicating that the emission mechanism at these burst phases may be thermal at variance with the apparently non-thermal emission during the main gamma-ray event.

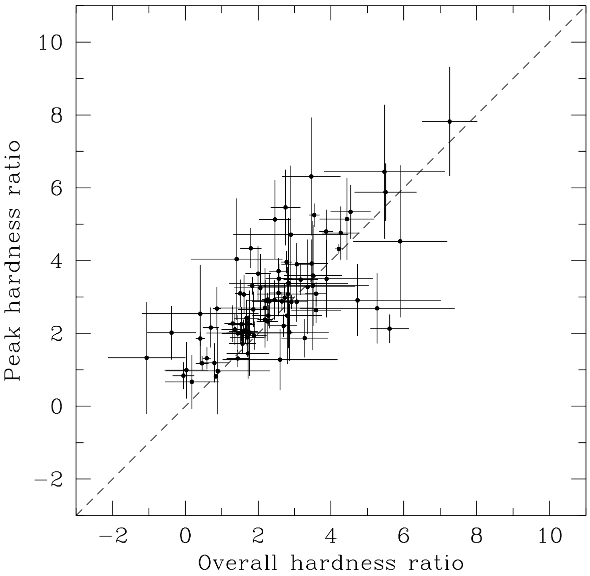

Fig. 5. Burst peak hardness ratios vs. burst overall hardness ratios. The dashed line indicates the case of equality of these two quantities

Table 2. Gamma-ray bursts with precursor or tail X-ray activity

Burst name	Type of X-ray activity
W900222	precursor and tail
W900708	precursor and tail
W900901	tail
W910817	tail
W911209	precursor
W920718	precursor
W920723b	tail
W920903	tail
W920903b	precursor
W920925	precursor
W921013b	tail
W921022	tail
W930705	tail

4.4. Distribution of bursters in space

For describing the distribution of GRB sources in space, the V/V_{max} statistics (Schmidt et al. 1988) is widely used. In this statistics, for each burst detected according to the set criterium one calculates the quantity V/V_{max} by the formula: $V/V_{max} = (C_{max}/C_{min})^{-3/2}$, where C_{min} is the minimum count rate to satisfy the burst detection criterion, and C_{max} is the maximum count rate during the burst. If the bursters are homogeneously distributed in space, V/V_{max} will be uniformly distributed in the interval (0,1), and its expectation will be 0.5.

We have carried out a V/V_{max} test on the WATCH GRB catalogue. Calculating the values of the parameters C_{min} and C_{max}, in order to have a homogeneous sample, we used the count rate data with 14 s integration time, for data of such resolution exist for all of the events. Of crucial importance in our case is the definition of C_{min}, since the inclusion of many bursts into the catalogue was dependent on observations of the event by other experiments. We have chosen the criterion that the peak count rate must exceed the background by at least $\sim 15\sigma$ (this limit very roughly corresponds to a flux threshold of $\sim 3 \times 10^{-7}$ erg cm^{-2} s for the WATCH sensitivity energy range and a typical trigger time scale of 8 s), for it proves that virtually all cosmic bursts meeting it can be registered with WATCH independently, through localization. The average value of V/V_{max} for 43 so selected events is 0.54 ± 0.04. This implies that the burst sources are homogeneously distributed within the WATCH sampling distance. The WATCH instrument is not sensitive enough to make it possible for us to analyze the distribution of more distant bursters, a deficit of which has been observed in a number of burst experiments (Meegan et al. 1996; Terekhov et al. 1995).

4.5. Burster locations in the sky

The location of the source of a burst can be found from the WATCH data if the following three requirements are met: 1) the burst is strong enough, 2) it lasts longer than ∼ 1 rotation of the modulation collimator, and 3) the modulation pattern used for localization is not significantly distorted by the presence in the light curve of bright details on time scales shorter than the rotation period of the collimator. The presence of other bright sources in the field of view can possibly make the procedure of deriving the source position unreliable even when the above conditions are satisfied. Therefore we considered a source localized only if the same position was resulted from two statistically independent modulation patterns. These patterns may belong to different time intervals, different energy ranges, or, in rare cases, different phase intervals of the same modulation pattern. For several weak bursts an additional independent verification was obtained through comparing the positions provided by WATCH and BATSE.

We have succeeded in localizing the sources of 47 bursts (Table 3). The statistical uncertainty of position determination is inversely proportional to the significance of source detection and varies between 7 arcmin and 1.5 deg for the localized bursts (the radius of a circle with an area equal to the area of the 3σ confidence region), the localization region being an ellipse somewhat contracted along the source off-axis angle θ. In preparation of this catalogue special efforts were made to decrease the influence of various systematic effects on burst localizations. Significant progress in this direction has now been achieved, in the first instance due to the use of information provided by the star tracker of the SIGMA telescope for determination of the attitude of the spacecraft at the times of bursts. Besides, on the basis of an ample archive of WATCH data on localizations of bright persistent X-ray sources, we have found more accurate values for some of the parameters relevant to the instrument, including the mounting angles defining the orientation of the WATCH detectors with respect to the SIGMA star tracker. Unfortunately, the star tracker was at times off during WATCH observations, and for 16 bursts we thus were bound to use other information resources to calculate the attitude, namely readings of the navigational instruments of the spacecraft and the knowledge of the celestial positions of bright X-ray sources that are always present in the field of view and can be localized with the WATCH detectors. This leaves an irremovable uncertainty $\sim 0.5^\circ$ resulted from the rapid ($\sim$ 30 min period) and virtually unpredictable wobbling of the spacecraft attitude. For the 31 positions that were calculated using precise navigational information we conservatively estimate the remaining systematic error at 0.2°. This uncertainty is mainly due to the not complete accounting for various physical phenomena in the instrument mathematical model currently used, in particular the dependence of the instrument's positional response on the energy spectrum of the incident radiation. The cumulative localization uncertainties given in the last column of Table 3 were calculated by summing (in quadrature) the statistical (3σ) and estimate systematic errors. Although we have already arrived at the state that for most of the localized burst sources it is the statistical error that mostly contributes to the location uncertainty, a cooperative effort between IKI and DSRI is now in progress to further improve the modelling of the instrument, which we expect will eventually enable further reducing of the localization regions of several stronger bursts.

When analyzing a celestial distribution of sources, it is necessary to know how long different regions of the sky have been monitored. We have compiled from the WATCH data an exposure map, which is shown in Galactic coordinates in Fig. 6. Calculating this map, in cases when a sky region had been observed simultaneously by two or three WATCH detectors, the corresponding time interval was appended only once. We considered an area of the sky being in sight of the instrument if it was not more than 65° off axis. The maximum of the exposure map of 510 days is located in the vicinity of the Galactic center ($l = -7^\circ$, $b = 3^\circ$), and its minimum of 218 days has coordinates $l = 87^\circ$, $b = 29^\circ$. The exposure time averages 372 days over the celestial sphere, which corresponds to an all-sky monitoring efficiency of 21 %.

In Fig. 7, a celestial map of the positions of the burst sources in Galactic coordinates is presented. In order to check the angular distribution of the bursts for possible large-scale anisotropies, we have calculated its dipole and quadrupole moments relative to the Galactic center and the Galactic plane, respectively. Upon correction for exposure time (terms are summed with weights inversely proportional to the position exposure) the dipole moment $< \cos\theta >= 0.10 \pm 0.08$ (θ is the source angular distance from the Galactic center), the quadrupole moment $< \sin^2 b - 1/3 >= -0.01 \pm 0.04$ (b is the source galactic latitude). Therefore our observations are consistent with an isotropic distribution of the burst sources on the sky, in agreement with the corresponding BATSE result (Meegan et al. 1996). We carried out similar calculations for samples of bursts selected out by various attributes. We have not found any significant deviations from isotropy, in particular, the distribution of the sources of the stronger bursts is apparently isotropic. Note that the dipole and quadrupole moments calculated using the 32 events of the first WATCH catalogue of GRBs are: $< \cos\theta >= 0.22 \pm 0.10$, $< \sin^2 b - 1/3 >= -0.04 \pm 0.05$, respectively (Castro-Tirado et al. 1994). Thus, the tendency for bursters to concentrate towards the Galactic center, evident at a significance of 2σ in the first catalogue, is not confirmed by the new data obtained since October 1992.

Table 3. GRANAT/WATCH localizations of gamma-ray bursts

Burst name	α (2000.0) (°)	δ (2000.0) (°)	l (°)	b (°)	3σ stat. error (°)	Total error (°)
W900118	174.68	-44.32	289.46	16.64	0.54	0.73
W900123b	357.19	-38.56	347.89	-72.61	0.60	0.78
W900126	131.15	-37.79	258.76	3.09	0.24	0.32
W900222	336.73	34.83	92.09	-19.25	0.79	0.81
W900708	185.91	30.62	181.40	82.99	0.22	0.30
W900708b	252.79	16.20	34.92	33.74	0.43	0.48
W900901	276.31	-45.18	349.28	-14.59	0.45	0.67
W900925	133.14	-36.72	258.92	5.00	0.77	0.80
W900929	169.68	-6.48	265.83	49.59	0.44	0.49
W901009	348.61	30.40	99.28	-27.98	0.51	0.72
W901116	39.93	24.97	151.95	-31.73	0.48	0.52
W901121	30.39	72.40	128.24	10.26	0.55	0.59
W901219	348.62	-54.00	329.84	-57.77	0.55	0.59
W910122	297.48	-71.23	324.06	-30.26	0.66	0.69
W910219	212.94	58.54	104.43	55.61	0.93	0.95
W910310	184.10	6.38	279.48	67.64	0.24	0.55
W910627	199.60	-2.60	316.32	59.57	1.08	1.09
W910821	353.08	-72.01	311.26	-43.81	0.38	0.43
W910927	49.70	-42.72	250.24	-56.37	0.80	0.94
W911016	297.37	-4.71	35.35	-15.05	0.78	0.92
W911202	171.97	-22.59	278.81	36.34	0.80	0.94
W911209	261.92	-44.19	345.18	-5.15	0.60	0.78
W920210	154.15	47.89	167.78	53.51	1.08	1.19
W920311	132.25	-36.39	258.20	4.65	0.26	0.33
W920404	323.07	22.53	73.92	-20.85	0.63	0.66
W920714	221.43	-30.75	330.15	26.01	0.48	0.52
W920718	21.37	-3.36	143.31	-64.88	0.75	0.78
W920718b	296.17	-55.95	341.69	-29.51	0.62	0.65
W920720	145.67	-11.20	246.46	30.31	1.07	1.09
W920723b	287.08	27.33	59.26	8.69	0.19	0.28
W920814	259.83	-45.17	343.53	-4.47	1.13	1.24
W920902	279.08	-22.81	10.87	-7.04	0.41	0.46
W920903	295.87	35.46	70.02	5.81	0.67	0.70
W920903b	301.54	22.59	61.53	-5.05	0.22	0.30
W920925	201.11	42.20	100.96	73.49	0.73	0.76
W920925c	330.80	25.48	81.64	-23.60	0.34	0.39
W921013	87.97	1.93	204.27	-12.31	1.50	1.51
W921013b	117.71	33.41	186.99	26.20	0.25	0.32
W921022	254.43	-9.64	10.21	19.97	0.52	0.72
W921029	35.82	-0.42	166.28	-55.37	1.23	1.25
W930612	109.24	-71.20	282.48	-23.56	0.68	0.70
W930703	311.06	8.04	54.10	-20.65	0.59	0.77
W930706	281.42	-20.18	14.23	-7.83	0.42	0.47
W940419	358.82	-48.19	326.63	-66.27	1.00	1.02
W940701	145.67	-6.15	241.88	33.54	1.54	1.56
W940703	133.20	28.11	197.08	37.69	0.12	0.24
W940907	161.42	-31.81	273.93	23.88	0.84	0.98

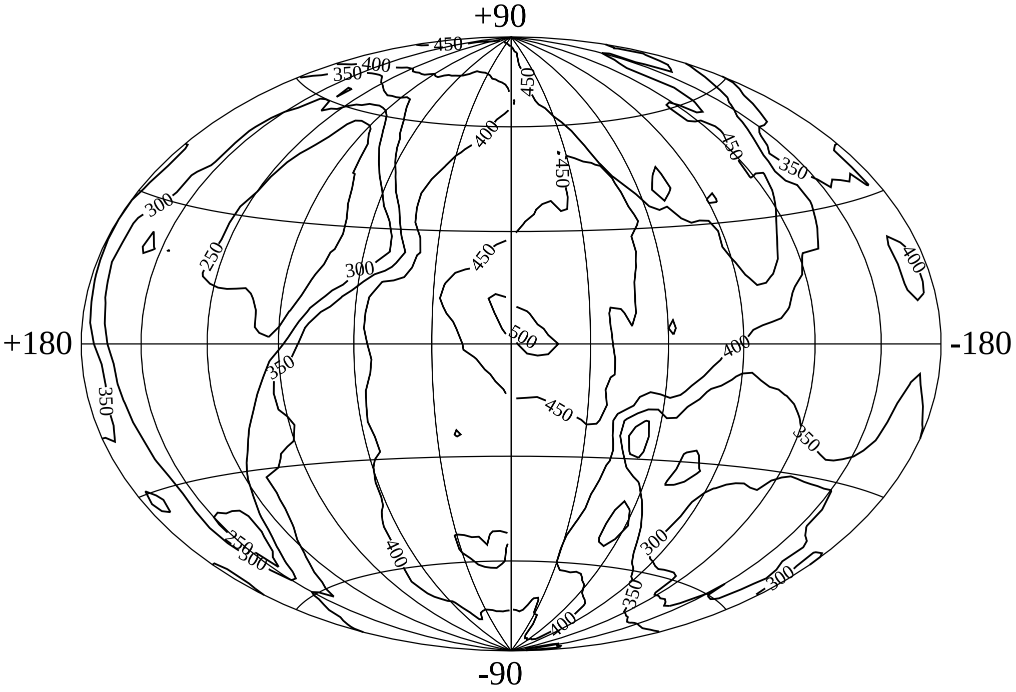

Fig. 6. Sky exposure map in Galactic coordinates constructed from the data of WATCH observations in 1989–1994. Exposure time is measured in days

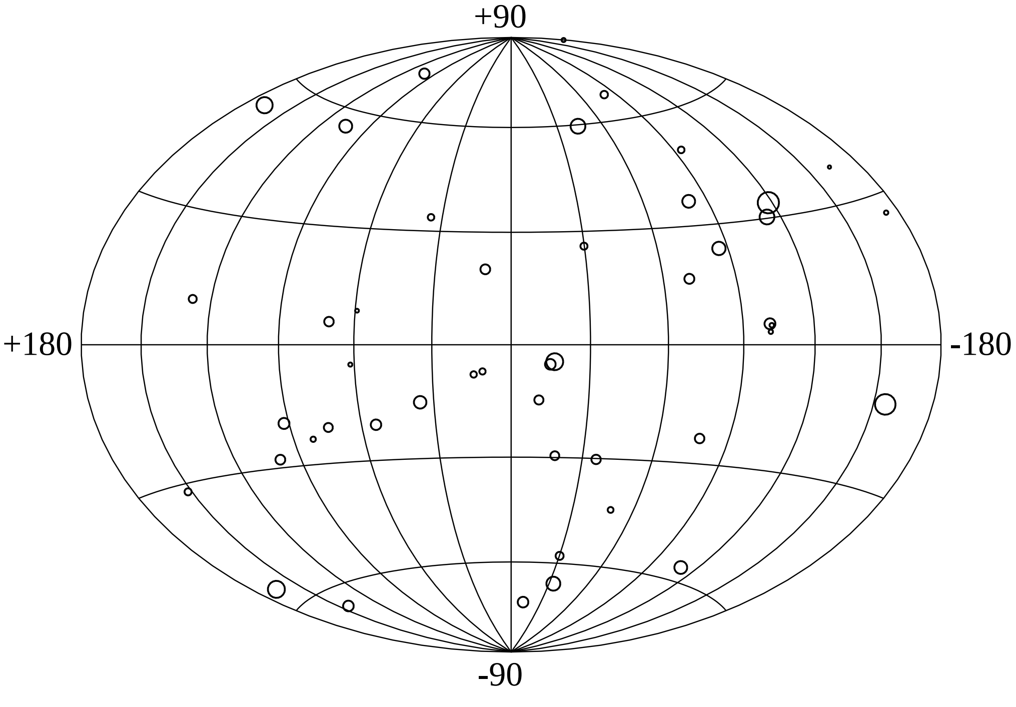

Fig. 7. Positions of 47 burst sources in the sky in Galactic coordinates. The circles shown are the twice-zoomed real localization circles

5. Summary

The WATCH GRB catalogue provides a set of 47 burster positions, 39 of which have a total (statistical plus systematic) uncertainty of less than 1 deg. For 13 events error boxes with radii smaller than 30 arcmin are now available. The WATCH sample thus contributes to the currently available list of moderately accurate GRB positions a number of locations comparable to that accumulated by the interplanetary satellite networks and never before obtained with any stand-alone instrument. We therefore hope that the new data presented here will be useful for burster counterpart searches in different energy ranges as well as for studying possible correlations in GRB positions.

The WATCH GRBs appear distributed both isotropically on the celestial sphere and homogeneously in space. These two results seem to be consistent with the implications from the third BATSE catalogue, as WATCH is about an order of magnitude less sensitive than the large-area detectors of BATSE, and the brighter bursts in the BATSE catalogue also show both isotropy and homogeneity (Meegan et al. 1996).

The light curves of most bursts observed by WATCH show hardening of the energy spectrum near the burst maxima. Several bursts demonstrate a significant 8–20 keV activity in the absence of hard X-ray flux either before or after the GRB. To all appearances, these X-ray events accompanying gamma-ray bursts are higher energy manifestations of the soft X-ray precursors and tails observed at 1.5–10 keV by GINGA.

Acknowledgements. We thank all specialists involved in the GRANAT/WATCH experiment, in particular: the staffs of the Lavochkin Association, the Evpatoria Deep Space Control Center and the group of B.S. Novikov maintaining the instrument operations; the group of A.V. Dyachkov at IKI RAN processing telemetry data; N.G. Havenson and E.M. Churazov for their assistance in determining the spacecraft attitude. The participation of the russian co-authors in this project was supported by Russian Basic Research Foundation grant No. 95-02-05938 and INTAS grant 93-3364. SS acknowledges the hospitality of the Max-Planck-Institut für Astrophysik where the final manuscript of this paper was finished.

References

Brandt S., 1994, Ph. D. Thesis, University of Copenhagen

Brandt S., Lund N., Castro-Tirado A.J., 1994. In: Fishman G.J., Brainerd J.J. and Hurley K.(eds.) AIP Conference Proc. 307, Gamma-Ray Bursts. AIP, New York, p. 13

Golenetskii S.V., Aptekar R.L., Gurian Y.A. et al., 1991, SvA 17, 195

Castro-Tirado A.J., 1994, Ph. D. Thesis, University of Copenhagen

Castro-Tirado A.J., Brandt S., Lund N. et al., 1994. In: Fishman G.J., Brainerd J.J. and Hurley K.(eds.) AIP Conference Proc. 307, Gamma-Ray Bursts. AIP, New York, p.17

Hanlon L.O., Bennett K., Collmar W. et al., 1994, A&A 285, 161

Hurley K., Lund N., Brandt S. et al., 1994. In: Fishman G.J., Brainerd J.J. and Hurley K.(eds.) AIP Conference Proc. 307, Gamma-Ray Bursts. AIP, New York, p. 364

Kouveliotou C., Meegan C.A., Fishman G.J. et al., 1993, ApJ 413, L101

Lestrade J.P., Dezalay J.-P., Atteia J.-L. et al., 1993, A&AS 97, 79

Lund N., 1986. In: Culhane J.L.(ed.), SPIE Proc. 597, X-ray Instruments. Int. Soc. for Optical Eng., Bellingham, Washington, p. 95

Meegan C.A., Pendleton G.N., Briggs M.S. et al., 1996, ApJS 106, 65

Murakami T., Inoue H., Nishimura J. et al., 1991, Nat 350, 592

Murakami T., Ogasaka Y., Yoshida A. and Fenimore E.E., 1992. In: Paciesas W.S., Fishman G.J. (eds.) AIP Conference Proc. 265, Gamma-ray Bursts. AIP, New York, p. 28

Ogasaka Y., Murakami T., Nishimura J. et al., 1991, ApJ 383, L61

Schmidt M., Higdon J.C., Hueter G., 1988, ApJ 329, L85

Sunyaev R.A., Churazov E.M., Gilfanov M.R. et al., 1993, ApJ 402, 579

Terekhov O.V., Denisenko V.V., Lobachev V.A. et al., 1994, SvA 20, 323

Terekhov O.V., Denisenko V.V., Lobachev V.A. et al., 1995, SvA 21, 83

This article was processed by the author using Springer-Verlag LaTeX A&A style file *L-AA* version 3.

Table 1. Basic information on GRANAT/WATCH gamma-ray bursts

Burst name	Start (UT)	T_{90} (s)	Fluence (10^{-7} erg/cm^2)		Hardness ratio	Peak flux (10^{-7} erg/cm^2/s)		Rem	Confirm[a]
			8–20 keV	20–60 keV		8–20 keV	20–60 keV		
W900118	17 40 06	227±27	102.1±4.9	169±11	1.65±0.14	0.87±0.10	1.81±0.23		
W900120	20 37 51	61±16	28.3±4.2	65.3±9.2	2.31±0.48	0.67±0.13	1.91±0.30	b	K
W900123	01 42 17	7.5±6.5	8.6±1.1	13.2±2.6	1.54±0.37	0.63±0.09	1.41±0.21	b	K
W900123b	18 44 31	15±10	25.3±3.5	40.6±8.1	1.60±0.39	1.01±0.10	2.08±0.26		
W900126	18 04 22	22.6±1.2	79.7±1.5	67.3±2.9	0.84±0.04	18.95±0.52	15.60±0.79		G
W900222	11 56 34	246±38	110.8±5.2	44±14	0.41±0.13	1.73±0.10	3.21±0.27		Ph
W900308	09 39 09	29±18	4.7±2.2	13.7±3.8	2.9±1.5	0.16±0.06	0.76±0.11	b	KPh
W900404	17 54 35	0.38±0.04	1.04±0.20	6.14±0.56	5.9±1.2	7.5±2.9	34.2±8.2	b	PhS
W900413	10 11 30	37±15	–	–	–	–	–	b	Ph
W900618	23 12 24	73±20	17.2±3.3	59.5±7.2	3.46±0.80	0.46±0.11	2.93±0.26	b	Ph
W900708	11 28 10	181±27	108.9±8.1	279±17	2.56±0.25	2.57±0.20	9.49±0.48		
W900708b	18 44 54	94±12	59.9±5.0	183.2±8.8	3.06±0.30	0.87±0.14	2.48±0.26		
W900901	01 33 40	195±12	38.9±4.3	176.9±8.6	4.54±0.55	0.74±0.09	3.99±0.22		
W900925	20 25 22	45.9±2.2	33.6±3.0	43.6±6.5	1.30±0.23	3.22±0.48	7.3±1.1		Ph
W900929	01 49 26	159.4±2.6	76.8±4.6	188±10	2.45±0.20	3.22±0.45	9.3±1.1		Ph
W901009	00 15 48	14.6±3.7	11.7±1.8	52.0±3.7	4.44±0.75	1.85±0.37	9.55±0.93		
W901015	08 44 46	–	12.8±2.9	28±15	2.1±1.3	0.67±0.11	1.80±0.64	b	Ph
W901027	04 21 01	13.2±9.3	17.7±1.8	47.8±4.3	2.70±0.37	1.04±0.10	2.30±0.24	b	PhS
W901112	14 57 41	21.9±8.9	4.7±1.3	18.5±2.9	3.8±1.2	0.37±0.10	1.31±0.21	b	PhU
W901116	01 42 12	14.5±8.9	11.3±1.8	40.8±3.7	3.59±0.68	1.21±0.12	3.22±0.26		Ph
W901121	18 07 11	188±12	61.5±3.7	92.8±7.0	1.51±0.15	0.65±0.07	2.00±0.13		PhU
W901219	21 52 43	39±10	46.1±5.6	146±12	3.17±0.47	2.30±0.22	8.00±0.54	c	
W910117	00 58 13	51±12	18.6±3.4	102±24	5.4±1.6	0.73±0.14	4.6±1.0	b	PhU
W910122	15 14 00	94.8±7.1	–	–	–	–	–		GPPhSU
W910219	11 45 24	59.2±1.9	69.3±2.9	124±19	1.80±0.29	7.22±0.51	31.2±3.3		PU
W910310	13 02 03	37.10±0.80	77.8±3.1	301.4±8.3	3.87±0.19	4.71±0.50	22.6±1.4		PU
W910425	00 38 05	104±13	57±10	203±30	3.51±0.80	1.15±0.34	4.13±0.99		BCPU
W910517	05 02 38	37.1±6.4	59.0±4.3	193±34	3.28±0.64	3.06±0.20	5.7±1.5	b,c	PPhSU
W910627	04 29 23	14.8±2.4	48.1±3.1	69±20	1.44±0.44	10.38±0.89	20.8±4.9		BCPPhU
W910717	04 33 06	9.2±1.1	27.8±2.5	22±11	0.80±0.41	7.09±0.94	8.4±3.6		BGPPhU
W910717b	13 07 23	14.7±6.4	15.9±3.9	22±19	1.4±1.2	1.04±0.27	4.2±1.3	b	U
W910721	19 30 17	29.4±9.0	28.4±4.7	5±21	0.18±0.74	1.76±0.30	1.1±1.2		BU
W910814	19 14 38	–	–	–	–	–	–	d	BCGOPPhSU
W910815	12 34 25	36.6±8.9	74.8±5.4	-3±22	-0.05±0.30	2.56±0.24	2.14±0.93	b	GPh
W910817	17 09 25	17.6±9.7	20.6±2.7	-7±13	-0.38±0.68	4.16±0.61	8.4±2.8	b	PhU
W910821	10 33 42	73±12	106.9±7.8	179±34	1.68±0.34	2.53±0.26	6.1±1.1		GPhS
W910901	05 24 34	13±11	12.6±2.7	22±14	1.7±1.1	0.59±0.11	1.19±0.64	b	Ph
W910925	03 35 10	45±10	17.2±3.6	-18±17	-1.0±1.0	0.57±0.18	0.77±0.85		B
W910927	23 27 00	28.7±6.2	50.6±3.5	76±18	1.51±0.38	4.19±0.25	8.4±1.1		BDU
W911016	11 01 34	264±19	65.9±5.4	135±45	2.06±0.71	1.07±0.12	3.46±0.92		BDGPPhU
W911022	04 14 00	–	8.9±2.7	3±14	0.4±1.6	0.85±0.19	2.1±1.0		BU
W911202	20 28 51	16.5±1.1	69.6±2.1	152±13	2.19±0.21	6.24±0.52	14.8±2.9		BDPU
W911205	23 04 55	29.5±6.4	14.4±2.6	50±20	3.5±1.5	0.70±0.15	2.3±1.1		B
W911209	18 36 11	22.1±2.5	26.3±1.7	71.7±4.7	2.73±0.26	4.26±0.42	12.7±1.2		BUY
W920116	18 30 47	–	3.0±1.3	7.9±3.4	2.6±1.5	0.41±0.11	0.53±0.30		BP
W920130	00 28 36	287±10	136.8±6.3	80±15	0.59±0.11	1.31±0.15	1.73±0.35	c	B
W920210	09 53 52	36.1±6.2	25.8±2.6	89.6±7.3	3.47±0.45	1.06±0.14	4.12±0.41		BPhS
W920302	06 17 16	58.8±5.6	12.2±2.3	21.0±6.0	1.72±0.59	0.47±0.11	0.69±0.28		B
W920307	00 18 11	58.8±8.0	16.9±2.0	26.5±5.4	1.57±0.37	1.29±0.11	2.21±0.27		BU
W920311	02 20 26	29.0±6.2	86.7±4.1	252±13	2.91±0.21	5.05±0.23	14.48±0.73		BDPPhSU
W920325	17 17 37	51.7±3.3	31.3±1.7	50.5±4.4	1.61±0.17	2.46±0.30	7.56±0.92		BDPPhSU
W920404	13 11 45	2.5±1.0	9.19±0.95	28.1±2.6	3.06±0.42	3.67±0.42	14.3±1.3		BU
W920419	20 07 01	26±11	4.1±1.5	21.9±4.0	5.2±2.1	0.27±0.07	0.72±0.19		BU
W920615	14 24 58	–	6.7±1.7	5.9±9.5	0.8±1.4	0.79±0.17	0.76±0.93		B
W920711	16 09 17	80.2±8.9	83.7±5.9	357±34	4.27±0.52	2.11±0.20	10.0±1.2	b	BDPUY
W920714	13 04 33	28.9±5.1	30.8±1.7	81.8±3.2	2.65±0.18	1.59±0.11	4.60±0.24		BPPhSU

Table 1 (continued)

Burst name	Start (UT)	T_{90} (s)	Fluence (10^{-7} erg/cm^2)		Hardness ratio	Peak flux (10^{-7} erg/cm^2/s)		Rem	Confirm[a]
			8–20 keV	20–60 keV		8–20 keV	20–60 keV		
W920718	14 40 43	64.6±8.8	58.4±2.5	26±10	0.46±0.18	2.02±0.11	2.40±0.39		BU
W920718b	21 32 44	4.50±0.80	12.92±0.74	29.4±1.5	2.28±0.18	3.69±0.32	9.21±0.73		BPhU
W920720	05 53 20	117±20	41.9±3.2	94±10	2.25±0.29	0.72±0.10	1.69±0.30		BPU
W920723	01 00 49	32.7±8.0	–	–	–	–	–	d	BDPhU
W920723b	20 03 09	53.0±3.7	59.4±2.1	209.9±4.3	3.54±0.15	7.83±0.41	41.1±1.2		PPhSU
W920814	06 10 35	21.6±6.2	10.5±1.3	19.9±2.5	1.89±0.34	0.56±0.08	1.09±0.16		BEU
W920902	00 29 02	7.3±1.1	11.7±1.1	85.2±3.0	7.26±0.76	2.02±0.35	15.7±1.1		BDPhU
W920903	01 35 46	131.8±6.3	42.0±3.4	107.4±7.3	2.56±0.27	0.58±0.10	1.80±0.22		PhU
W920903b	23 29 01	23.8±1.9	61.5±2.4	171.3±6.0	2.78±0.15	6.99±0.45	27.7±1.3		PhU
W920925	20 30 42	57.1±6.8	22.2±2.7	44.5±5.5	2.00±0.35	2.23±0.38	8.13±0.97		PhU
W920925b	21 45 20	12.9±5.6	10.8±1.3	20.2±3.8	1.87±0.42	1.00±0.12	2.65±0.36		BU
W920925c	22 46 24	282.1±8.8	120.3±4.8	207±10	1.73±0.11	1.55±0.11	3.50±0.24		U
W921001	04 03 54	–	4.8±1.3	13.6±2.7	2.80±0.96	0.73±0.30	1.80±0.63		B
W921013	20 32 32	12.9±2.0	6.50±0.85	15.9±1.9	2.46±0.44	1.15±0.21	5.92±0.61		BU
W921013b	23 00 42	344.6±3.7	114.2±4.9	209±11	1.84±0.13	8.11±0.43	26.8±1.2		PhU
W921021	18 20 46	32.4±7.9	14.6±2.0	24.8±5.9	1.70±0.47	0.82±0.13	1.56±0.36		B
W921022	15 21 00	95±13	57.2±2.8	49.8±5.9	0.87±0.11	1.84±0.30	4.95±0.72		BEUY
W921025	13 55 40	21.6±8.8	4.3±1.9	20.3±3.8	4.7±2.2	0.36±0.10	1.04±0.21	b	PhU
W921029	12 38 05	80.1±8.9	18.8±2.1	27.1±5.0	1.44±0.31	0.90±0.09	1.18±0.18		BU
W930106	15 37 40	0.06±0.03	–	–	–	–	–	d	BDPhSUY
W930116	02 47 06	7.3±5.1	3.9±1.2	13.0±2.9	3.3±1.3	0.37±0.12	1.24±0.28		BU
W930609	10 07 30	50±15	6.4±1.9	18.2±3.6	2.8±1.0	0.28±0.09	0.96±0.18		BU
W930612	00 44 20	130±51	29.9±3.1	77.0±7.5	2.57±0.37	1.00±0.09	3.48±0.23		BCDMPhU
W930703	11 26 30	7.3±1.1	13.5±1.6	37.3±3.2	2.75±0.41	3.01±0.52	16.4±1.3		
W930705	12 39 18	152±29	36.1±3.8	25.3±7.4	0.70±0.22	0.45±0.08	0.99±0.16		BU
W930706	05 13 31	4.50±0.80	16.71±0.81	37.8±1.6	2.26±0.15	8.48±0.42	24.8±1.0		BMPhU
W930710	03 14 42	14.4±6.2	4.5±1.3	12.8±3.0	2.8±1.0	0.42±0.11	0.87±0.24		BU
W930714	16 13 04	14.4±8.8	–	–	–	–	–	d	BPhU
W930910	12 12 30	79.8±6.2	27.8±6.5	78±14	2.82±0.85	0.88±0.26	2.74±0.59		BU
W930927	04 18 15	50±11	11.4±1.6	25.4±4.7	2.21±0.52	0.59±0.08	1.70±0.23		BU
W940307	07 56 29	14.3±8.7	2.9±1.4	8.5±2.6	2.8±1.6	0.18±0.08	0.59±0.16		B
W940329	18 15 44	72±11	–	–	–	–	—	d	BU
W940419	19 11 07	84±10	59.5±3.5	213±12	3.59±0.30	2.02±0.14	6.21±0.49		BPhU
W940619	21 32 32	72±11	–	–	–	–	–		BCPhU
W940701	21 44 29	201±23	54.9±4.2	307±16	5.61±0.53	1.18±0.11	2.51±0.39	c	BU
W940703	04 40 55	45.6±7.9	239.2±4.6	1010±17	4.22±0.11	9.36±0.22	40.46±0.93		BPhSUY
W940711	18 14 10	32.4±5.6	11.1±1.9	0.2±6.6	0.03±0.60	0.53±0.11	0.53±0.40		B
W940907	20 36 20	26±11	20.9±2.6	115±10	5.50±0.85	0.95±0.10	5.62±0.43		
W940910	23 57 56	51±15	38.1±3.8	51±13	1.36±0.37	1.09±0.11	2.30±0.40		Ph

Notes:

[a] Bursts were also observed by other instruments: B-BATSE/CGRO, C-COMPTEL/CGRO, D-DMS, E-WATCH/EURECA, G-GINGA, K-KONUS/GRANAT, M-Mars Observer, O-OSSE/CGRO, P-PVO, Ph-PHEBUS/GRANAT, S-SIGMA/GRANAT, U-ULYSSES, Y-YOHKOH.

[b] Direction of burst arrival unknown.

[c] Burst superimposed on variable background. Values given for the parameters possibly in error.

[d] Burst source was either outside or at the border of the WATCH field of view according to the BATSE localization (Meegan et al., 1996).

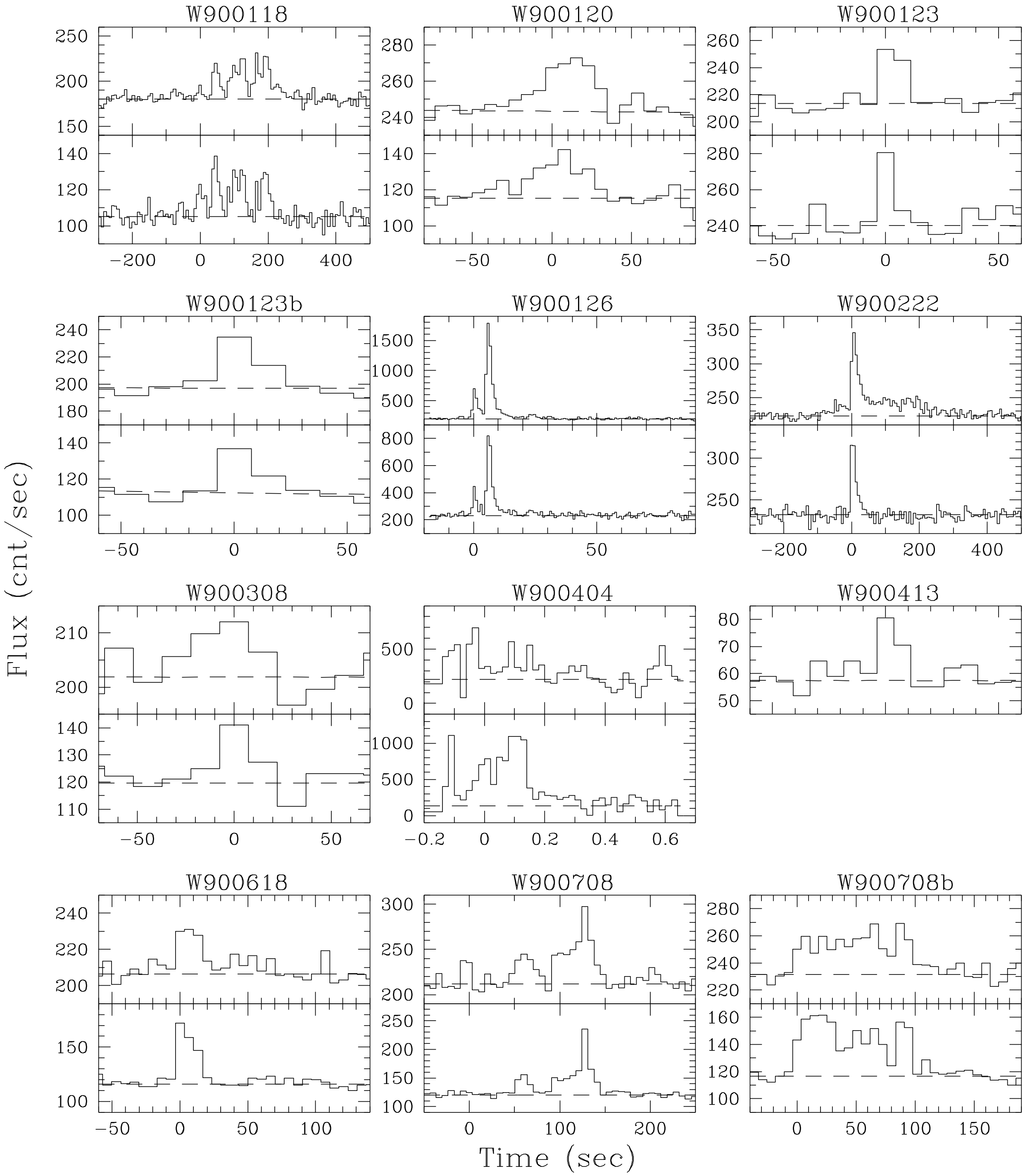

Fig. 2. Time histories of the gamma-ray bursts detected by WATCH in the two energy ranges: 8–20 keV (upper panels) and 20–60 keV (lower panels). Time runs relative to the burst start (see Table 1). The background count rate is indicated by the dashed line

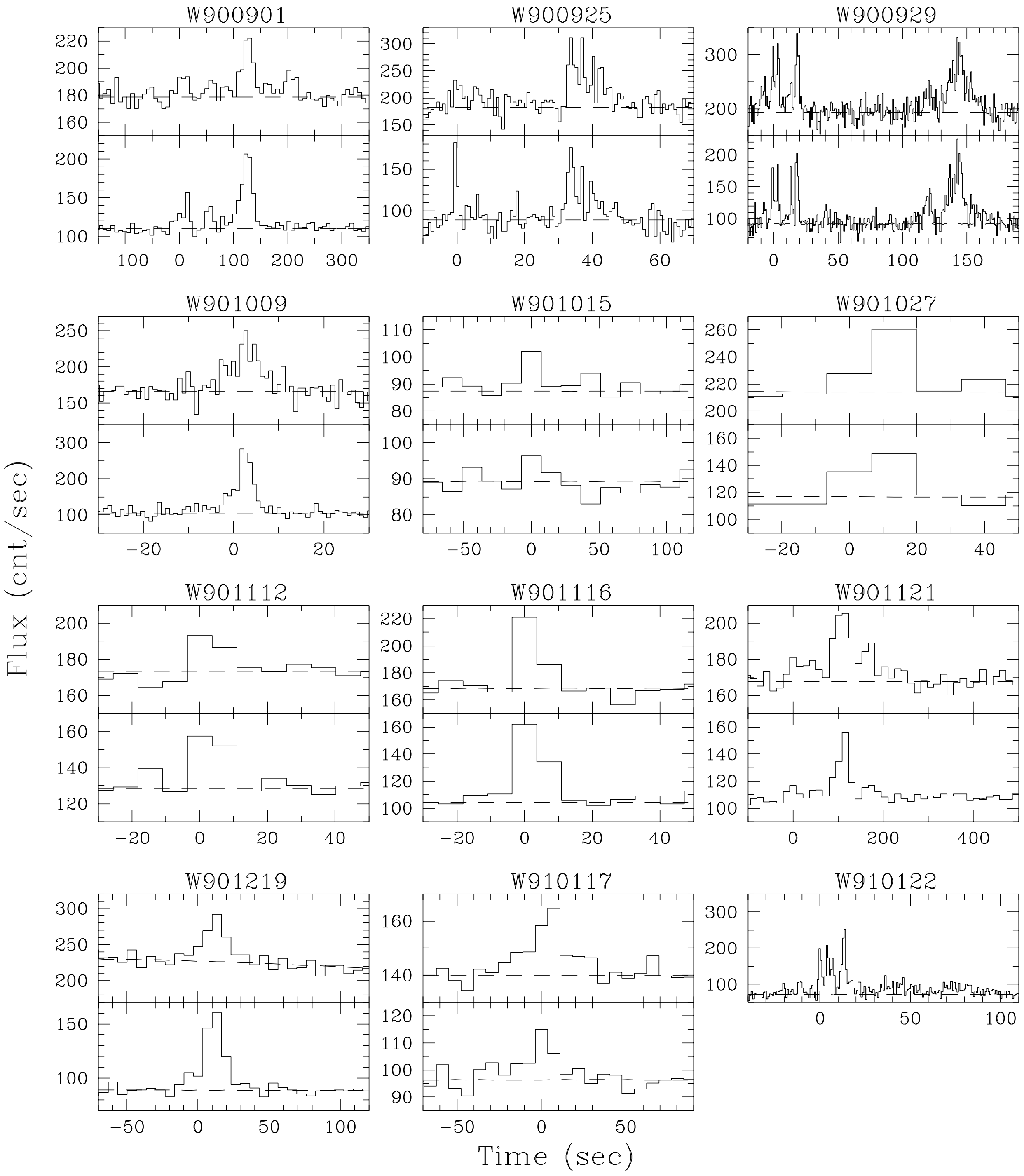

Fig. 2. continued

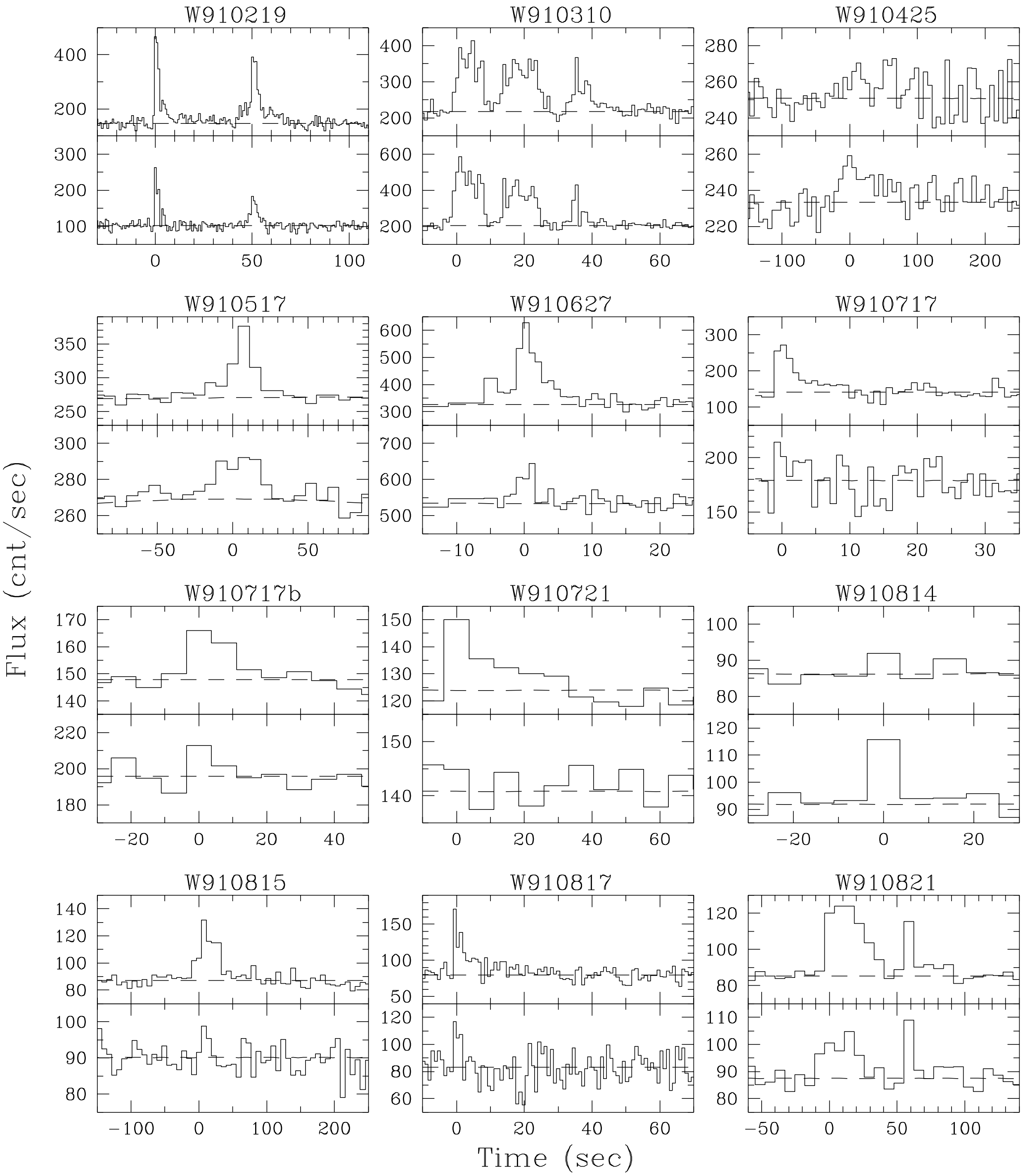

Fig. 2. continued

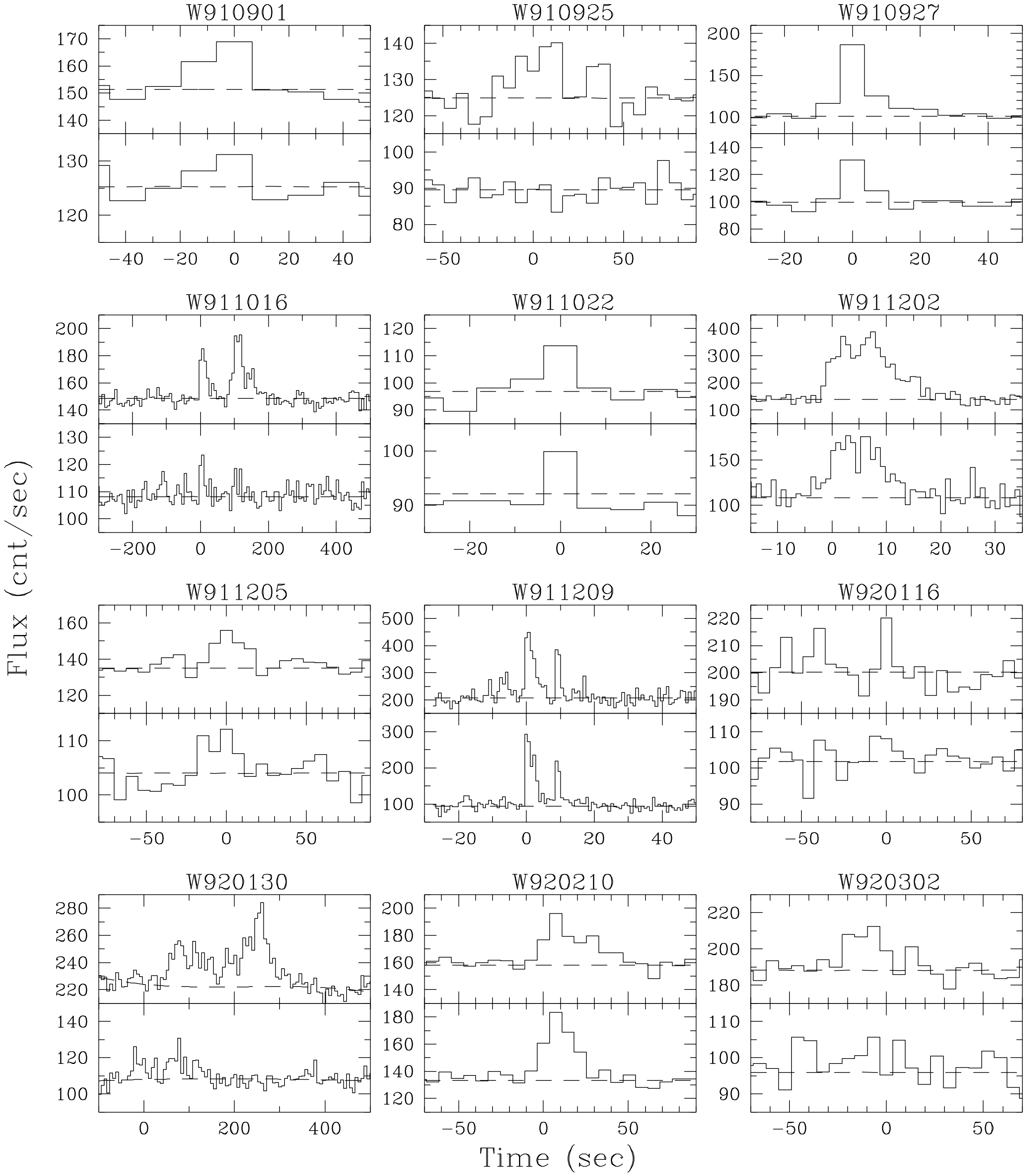

Fig. 2. continued

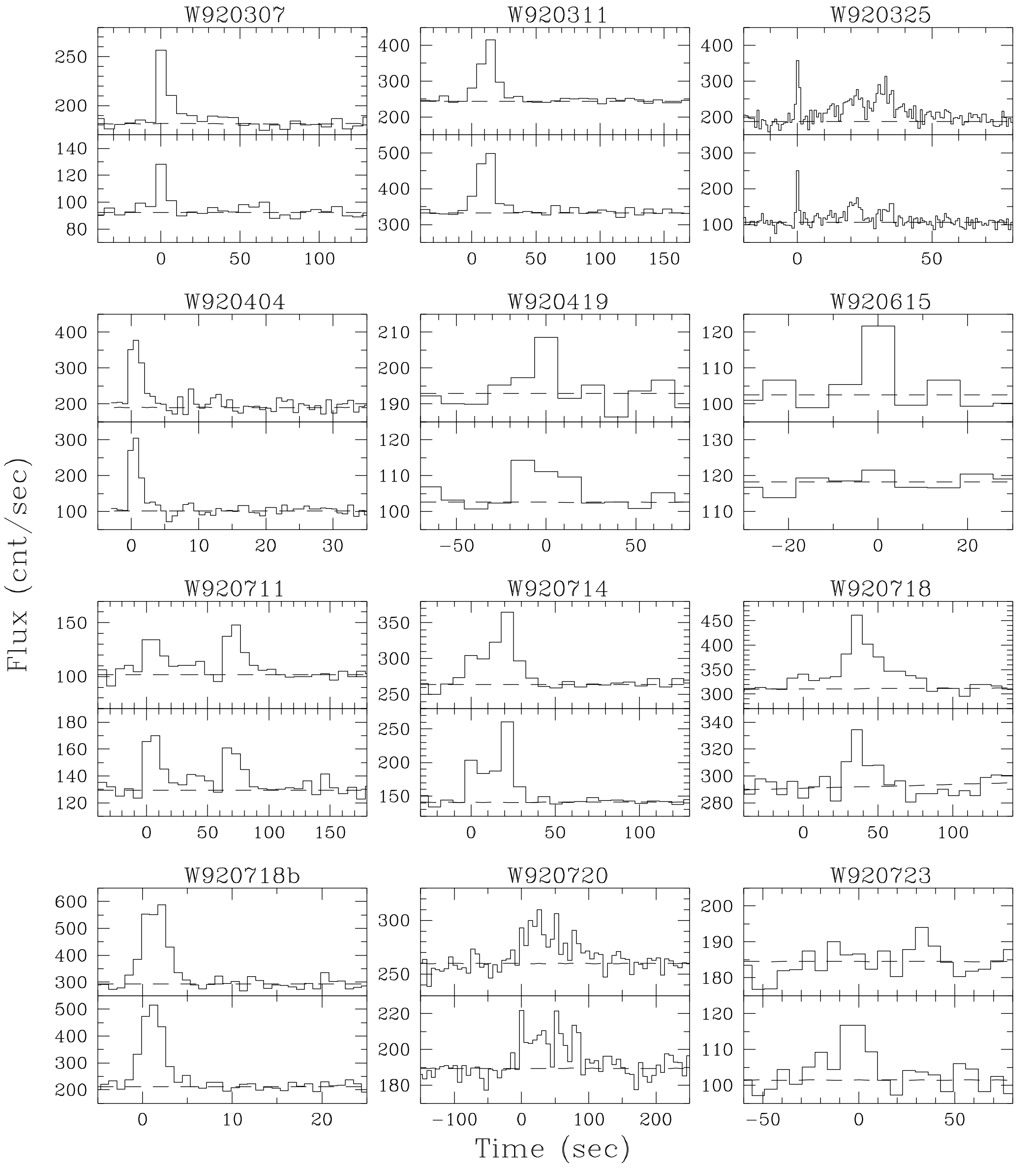

Fig. 2. continued

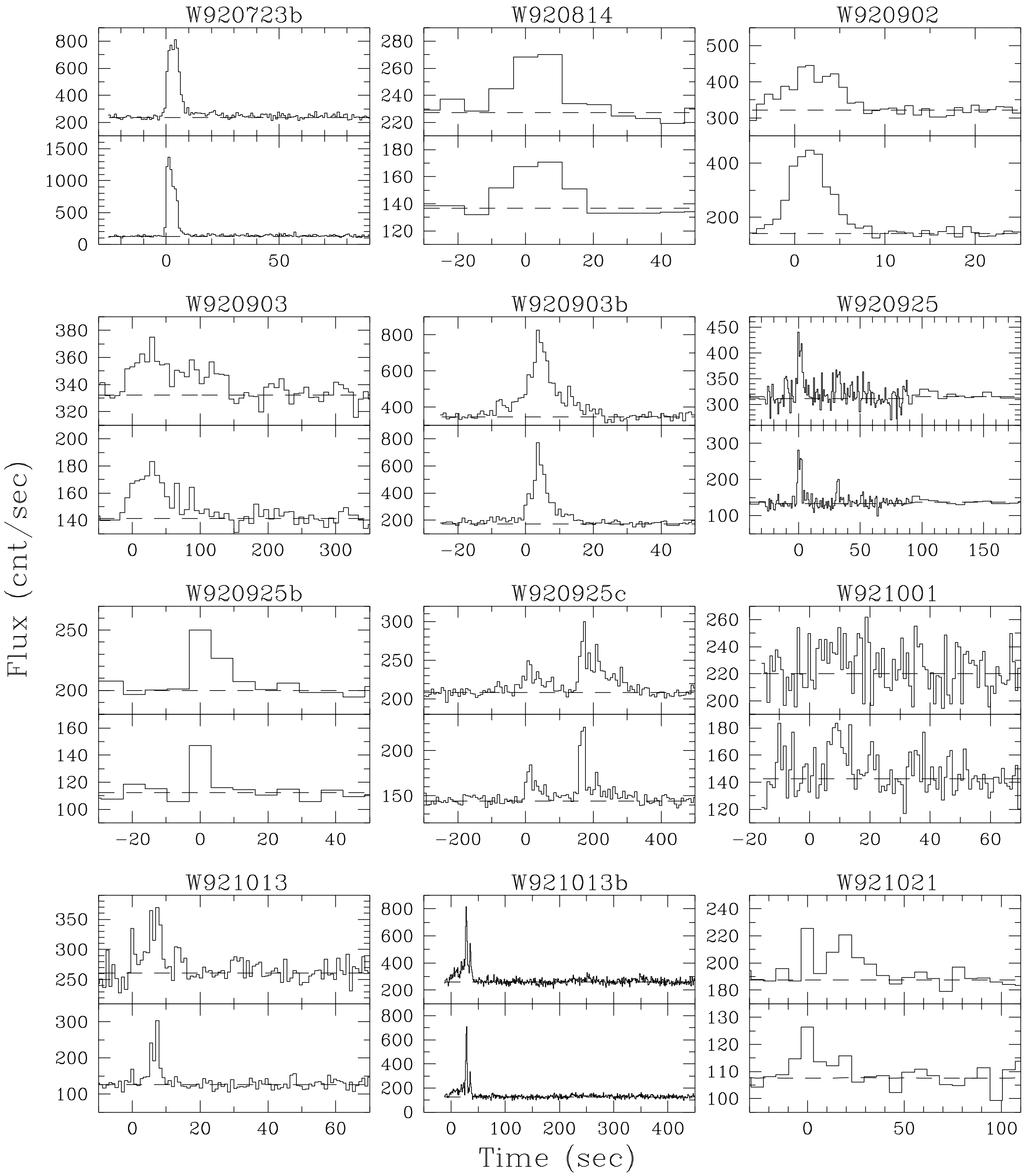

Fig. 2. continued

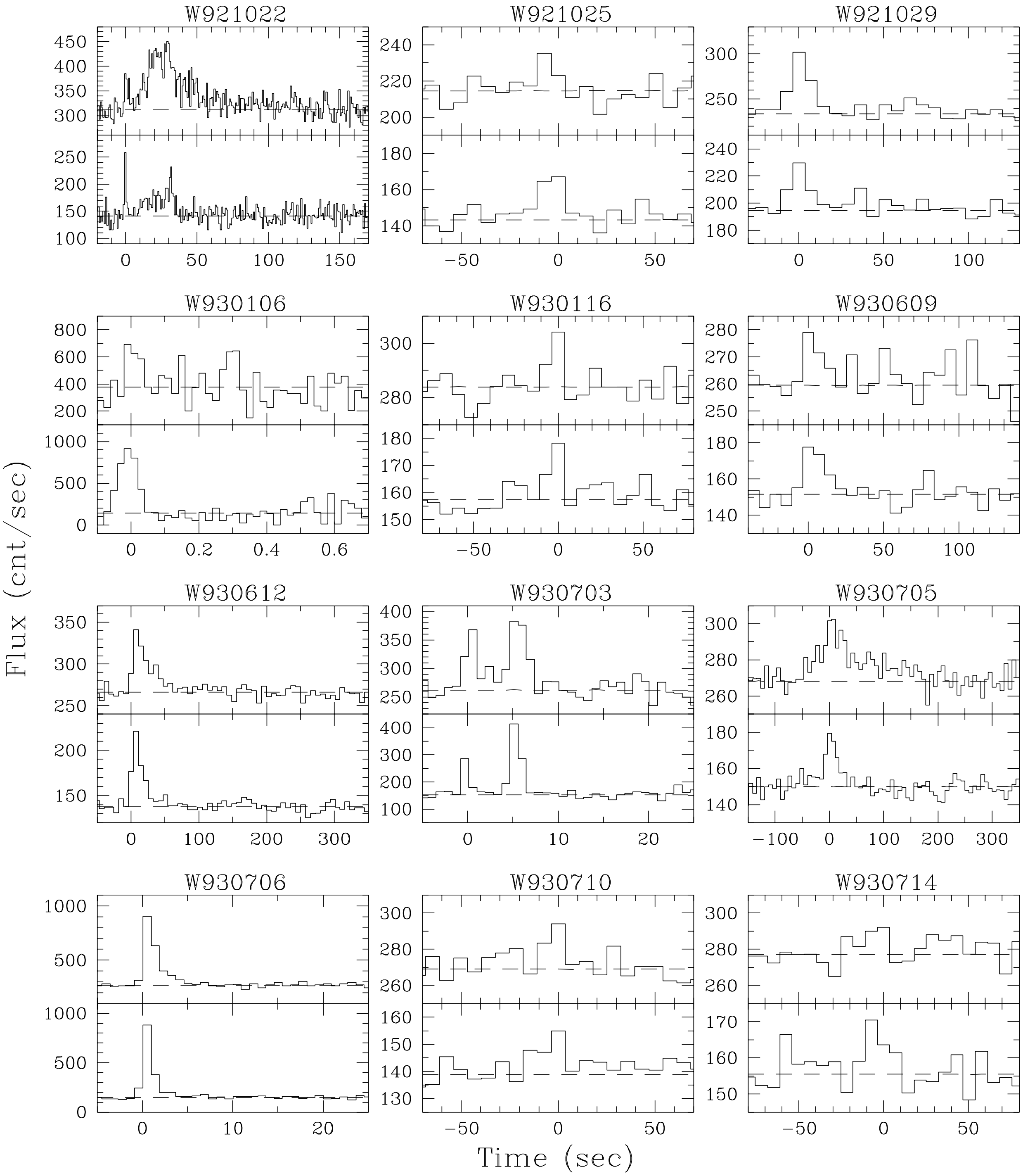

Fig. 2. continued

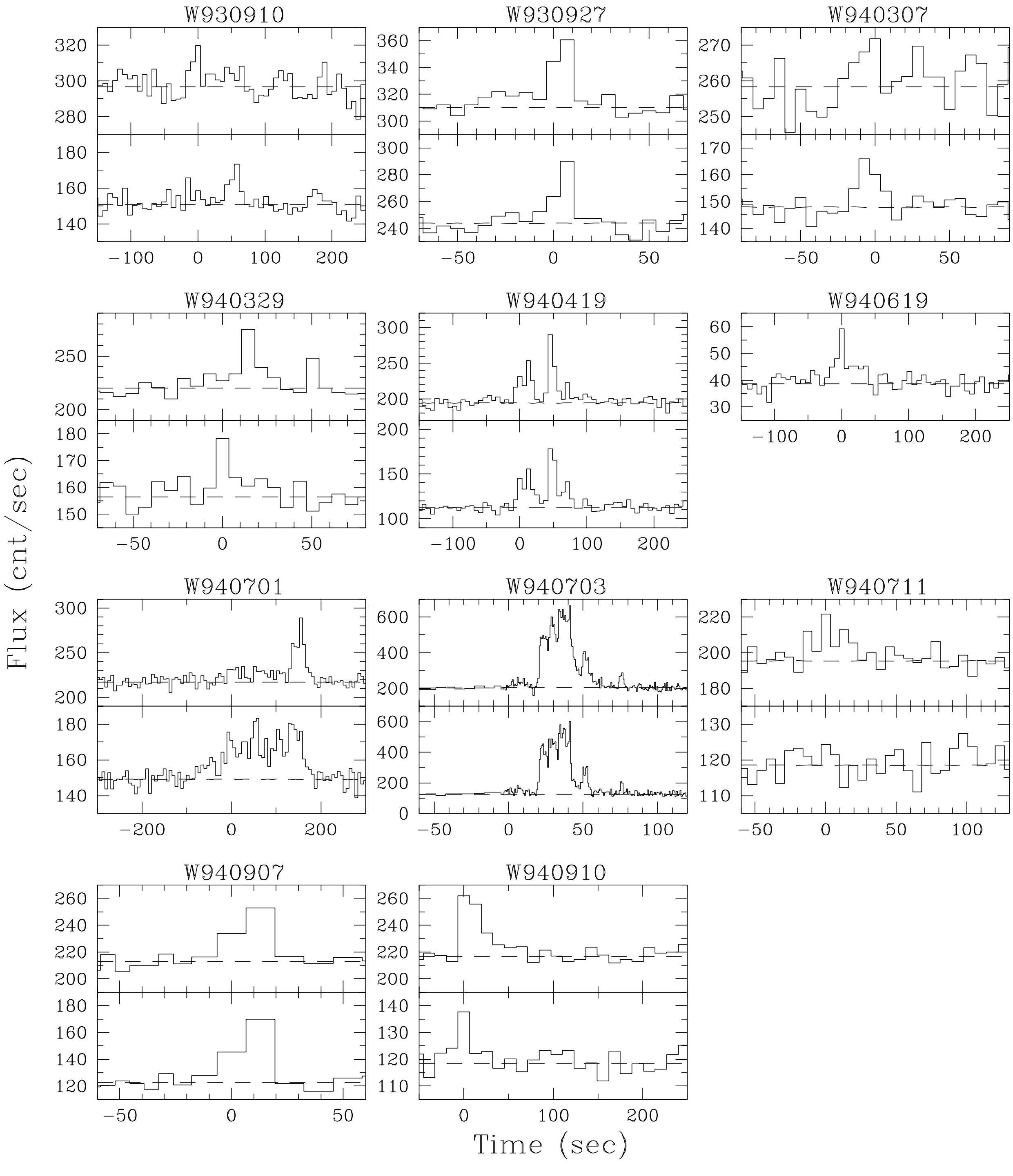

Fig. 2. continued